Modeling of Flexible Photovoltaic Modules on Irregularly Curved Surfaces

Abstract

The increased availability of thin film photovoltaic modules opens up possibilities for the application of flexible solar panels on irregularly curved surfaces. In order to efficiently arrange photovoltaic panels on such surfaces, geometric CAD tools as well as radiation analysis tools are needed. This paper introduces geometric methods that can help in the design of bendable panel geometry. By automating the generation of possible photovoltaic panel arrangements and linking the geometric tools to solar analysis software, we can analyse large numbers of design options in a relatively short time. The combination of geometry generation and solar analysis allows the optimisation of solar panel configurations for a category of panels for which such methods have hitherto not been available. The merits of the methods we introduce are illustrated with a case study, for which hundreds of design configurations have been explored in an automated manner. Based on analysis of the numeric data generated for each of the configurations, the effects of panel dimensions and orientation on geometric design considerations and solar energy yield have been established. The quantitative and qualitative conclusions resulting from this analysis have informed the final design of the photovoltaic system in the case study project.

1. INTRODUCTION

Designing structures that are optimised for structural efficiency [1] or tailored for digitally informed fabrication [2, 3] often results in complex geometry [4]. Typically this geometric complexity carries over to secondary building parts, for example roof systems. This creates design challenges, for which digital design and analysis tools are very suitable [5, 6].

Due to their rigidity and shape, most photovoltaic (PV) panels are difficult to apply in geometrically complex situations. However, thin film photovoltaic modules can be applied to thin sheet metal, creating bendable panels that can be used on non-planar base surfaces. Combined with the high efficiency and low weight of thin-film PV technologies such as CIGS (copper indium gallium selenide), this offers new application possibilities of PV modules, in particular for building integrated photovoltaics (BIPV).

Flexible sheet metal panels can be applied to surfaces with single curvature easily. However, when applying bendable panels to surfaces with double curvature, methods to predict the geometric behaviour of bendable panels are needed. As a major factor in the design of PV applications is solar insolation, integration with solar analysis tools is desirable.

Approximation of doubly curved surfaces by triangulation was already used in the pre-digital era in the context of sheet metal working [7], but this process was labour intensive and thus only suitable for lofted surfaces with few control curves, as shown in Figure 1 (left). This triangulation approach has gained broader application possibilities through its implementation in software. [8,9]

Many studies exist on the topic of placement and/or orientation of photovoltaic panels, but these typically focus on distributing and orienting flat modules over a flat horizontal surface [11, 12], or a flat vertical façade [13, 14]. In this paper we focus on design methods for placing bendable panels on irregularly curved surfaces by introducing a method that integrates automated generation of geometry with solar insolation analysis.

The geometric methods presented in [8] and [9] approximate a surface by triangulation and then unfold the triangles into a flat surface with a shape that is not known in advance. In our methods, we take the rectangular shape of unbent panels as a starting point and triangulate them in order to approximate the original surface. Methods presented in [10] also create strip-like surfaces, but allow deviations from exact rectangular shapes that are not permissible in the photovoltaic modules we employ.
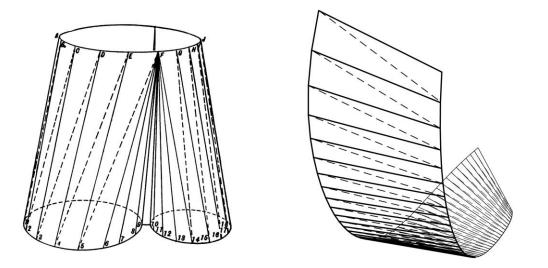

Figure 1. Left: Triangulation method described by Kidder [6]. Right: Our method.

The methods we developed have been applied to a pilot project, designing the configuration for a series of flexible photovoltaic panels on an irregularly curved roof shell. A large number of configurations with various panel dimensions and orientations were analysed.

In section 2, we start by introducing the methods to approximate doubly curved geometry using developable strips. After assessing the validity of these methods, we then discuss how the resulting geometry can be analysed on a number of metrics: total surface area, occurrence of bending, surface approximation accuracy and irradiance. Section 3 shows the application of the methods we developed on a case study building and discusses the results, focusing on the influence of various design parameters. Section 4 presents our conclusions.

2. METHODS

In this section, we introduce methods to generate strips of bendable photovoltaic panels by approximating a doubly curved surface using two different triangulation approaches (2.1–2.3), to efficiently arrange multiple of these strips on a larger surface (2.4) and to analyse the resulting geometry with regard to various geometric metrics (2.5) as well as solar insolation (2.6).

2.1. Panel generation method A: congruent triangle shapes

Our aim is to generate an approximation of a flexible panel that is bent over a doubly curved surface, following the surface as closely as possible while remaining developable and exactly resulting in a rectangle when unrolled.

As triangulated strips are perfectly developable, we decided to approximate the final shape of the photovoltaic panels by a series of triangles, of which all corner points lie exactly on the roof surface. The method to generate this geometry is shown in Figure 2.
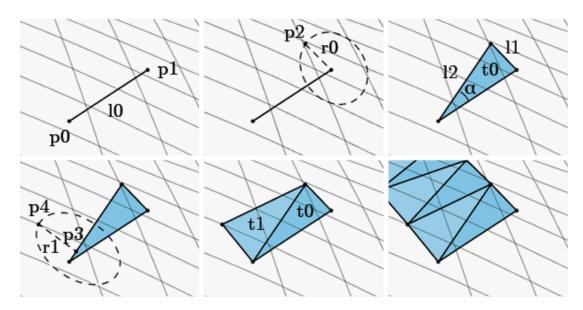
Figure 2: Surface approximation using congruent triangles (method A).

The following sequence of steps results in a regularly triangulated surface that approximates the base surface:

1. Create two points (p0, p1) on the base surface, such that the distance between them is the desired panel width (w) and the direction is perpendicular to the desired panel direction. Connect the points with a line (l0).

2. Create a circle with radius r0 around point p1, using a plane perpendicular to line l. Create a point (p2) at the intersection of this circle with the base surface.

3. Create two lines (l1, l2) connecting point p2 to points p0 and p1, thus creating triangle t0 with angle α at p0.

4. Create a point (p3) on l2 at distance $w \cdot \cos(\alpha0)$ from p2, then create a circle perpendicular to l2 around p3 using radius $w \cdot \sin \alpha$. Intersect this circle with the base surface, creating point p4.

5. Connect p4 with two lines to points p0 and p2, creating the triangle t1. Note that triangles t0 and t1 are congruent.

6. Repeat steps 2 - 5 as many times as necessary.

2.2. panel generation method B: adaptive triangle shapes

Although the method described in 2.1 does work for strips with changing curvature direction, it deals better with curvature along the length of the strip than with curvature perpendicular to that direction. In order to minimise the surface deviation of the triangulated strips, we tested a second triangulation method that deals better with situations where the main surface curvature direction is close to perpendicular to the panel's length direction. This method is shown in Figure 3.
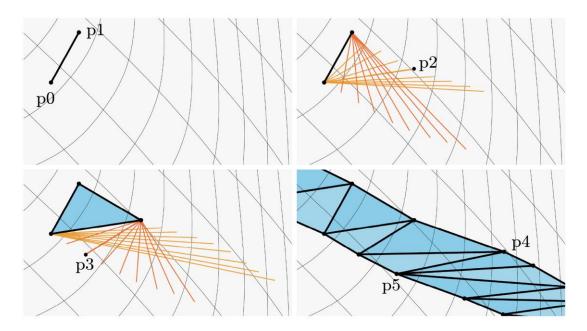

Figure 3: Surface approximation using adaptive triangle shapes (method B).

The following sequence of steps results in an irregularly triangulated surface that approximates the base surface and exactly unfolds into a rectangle:

1. Create two points (p0, p1) on the base surface, such that the distance between them is the desired panel width (w) and the direction is perpendicular to the desired panel direction. Connect the points with a line.

2. Create a series of lines starting at p0 and ending at points on the surface with distance $n \cdot d$ from p1 and $Sqrt((n \cdot d)^2 + w^2)$ from p0, where n is the number of lines and d is a distance that can be chosen at will. Create a second series of lines starting at point p1. Select the line that has the smallest distance between its midpoint and the base surface and call the endpoint of this line p2.

3. Draw a triangle using points p0, p1 and p2.

4. Continue creating triangles by repeating steps 2 and 3. Note that in some cases, more than two diagonal lines meet in one point, such as point 5 in Figure 3.

5. The end of the strip is a special case: if an exact strip length is desired, the value for distance d in step 2 should be set to the remaining edge length divided by an integer (which may be chosen at will). Once one of the corner points of the strip has been reached, potential end points can be created on the panel's short edge.

2.3.   Assessment of panel triangulation methods

In order to assess the extent to which triangulation methods A and B reflect actual bending behaviour of sheet metal, we created a physical model. Additionally, we studied the effect of changing the diagonal direction in method A, and we compared the geometric differences between methods A and B.
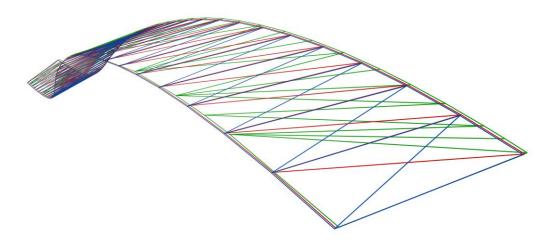

Figure 4: Comparison of triangulation methods A (blue, red) and B (green).

In a test of 46 triangulated strip segments generated with method A, the median lateral deviation between strips using different diagonal directions turned out to be 0.14% of the strip length. In the most extreme case, the lateral deviation was 2.1%.

Comparing method A with method B, the median lateral deviation on our test geometry is 0.20%. The most extreme deviation occurring is 3.7%.
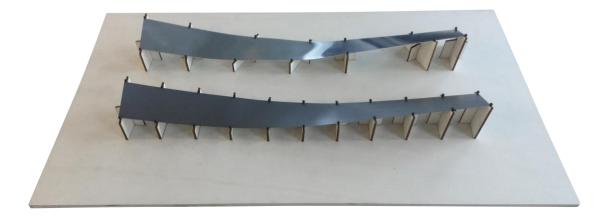
Figure 5: Scale model showing metal strips bent over edges created with methods A (bottom) and B (top).

Two scale models were created to test the sheet metal strip behaviour: one supported by elements perpendicular to the strip direction (generated with method A), and one supported by elements oriented roughly along the main curvature direction (using a subset of edges generated using method B).

Once mounted, the metal strip follows the predicted trajectory accurately in both models, as shown in Figure 5. Deviations turned out to be smaller than the thickness of the supporting material, which suggests that the digital approximation is a good representation of the bending behaviour of sheet metal.

An observation relevant to the fixation method of the panels is that perpendicular supports visibly deform the metal surface in areas of concave curvature, except when the main curvature direction is aligned with the strip. To avoid this visible deformation, the supports for the final panels can be aligned to the local curvature direction of the strips.
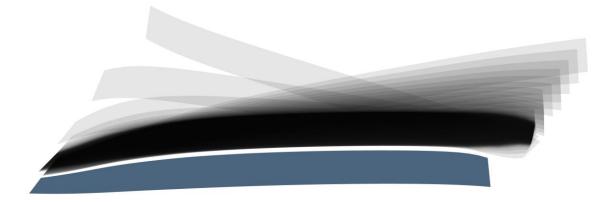
Figure 6: A series of potential neighbour panels (in grey) for an existing panel (in blue).

Figure 7: A potential neighbour panel. The length of the new panel and the distances d1 and d2 are used to determine the new panel's suitability.

2.4. Geometric method for strip arrangement

Using the methods shown in sections 2.1 and 2.2, single strips can be generated. In order to cover a larger area, we need to find a method to arrange multiple strips. To maximise solar insolation, we are looking for a solution that fits as many panels as possible. As an additional architectural constraint, we choose to only look at solutions where multiple panels are arranged in long strips. For installation purposes, these strips should spaced at a certain minimal distance.

On a surface with double curvature, strips that are parallel to each other at one position will diverge or overlap elsewhere. We aim to avoid overlapping and to keep strips roughly parallel to each other, so that the unused area between panels is minimised.

At any point along the length of a strip, a parallel strip can be created by taking the direction of the closest point in the existing strip as the start direction, as illustrated in Figure 6. In order to pick the best panel out

of the generated options, we use a formula favouring long neighbour strips and small differences between the gap sizes near the ends of the panels:

$$\text{suitability} = \frac{L}{\sqrt{c - min(d1, d2)/max(d1, d2)}} \qquad (1)$$

In this equation, L is the length of the new strip and d1 and d2 are distances between two strips at both ends (see Figure 7). Constant c should be larger than one as otherwise very short strips would be favoured over significantly longer, but slightly less parallel strips. For this analysis, we set c to 1.1.

By applying this method iteratively until the roof edge has been reached, large irregular surfaces can be covered with strip geometry, as illustrated in Figure 8.
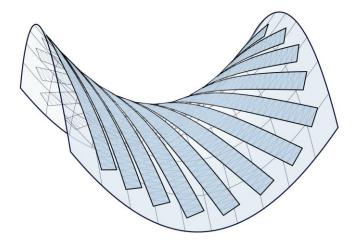

Figure 8: A series of strips approximating a hyperboloid surface.

2.5.   Calculation of bending and of surface approximation accuracy

The amount of module bending and the accuracy of surface approximation are important metrics as they strongly influence buildability, detail design and visual appearance.

We calculate approximate panel bending radii at every point along the strip edges by determining the angles between sets of three consecutive edge points. Radii that are close to or shorter than a user defined minimum radius are marked red in the graphical output (see Figure 9, left).

In order to get an estimate of the geometric deviations between the original surface and the generated strips, we measure the distance between various points of the strip geometry and the nearest points on the original surface. As all points on both sides of the generated strips lie exactly on the base surface, the points with

the largest surface deviation lie very close to the centre line of the strips, except when the bending radius of the base surface is smaller than half the strip width. As with the bending radii, this surface approximation accuracy is exported both graphically (see Figure 9, right) and numerically.
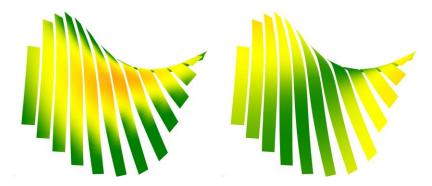

Figure 9. Left: Graphical display of the amount of bending; green indicates a large bending radius. Right: Graphical display of surface deviation at the center curve of the strips; green indicates a small deviation between the original surfaces and the triangulated strips.

2.6. Calculation of solar insolation

The power output of all generated panel configurations has been analysed using EnergyPlus [15] through the DIVA [16] and Ladybug [17] plugins for Grasshopper [18]. As weather data source, we used IWEC data for Geneva [19]. Using custom C# scripts, both graphical and numerical output were generated. Sun paths generated with DIVA were then used to visually study shadow occurrence on the roof, using the physically based render engine LuxRender. [20]

3. RESULTS

The methods developed in section 2 have been applied in the context of the design of the NEST Hilo building at EMPA Duebendorf, which is a test bed for novel building technology [21]. The building features a doubly curved roof, the shape of which is defined by structural considerations and a scaffolding process using textile formwork [22]. Photovoltaic cells mounted on thin, bendable metal plates will be placed on top of this roof, arranged in long parallel strips as shown in Figure 10. Our first aim is to assess the potential energy performance of various shell shapes and thus provide design feedback from an energy production perspective. Our second aim is to define panel dimensions and a panel arrangement on the final

roof shell in a way that results in a high PV solar insolation, while in parallel fulfilling architectural and technical requirements.
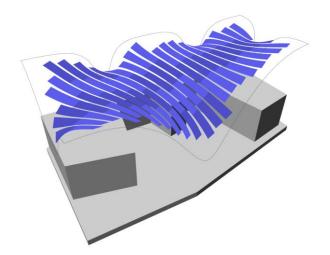

Figure 10: Model of a series of bent photovoltaic panels placed on the Hilo building roof.

3.1.   Comparative analysis of various roof shell shapes

When comparing a series of seventeen roof shapes, the solar insolation per square meter varied by about 8% between the best and the worst roof shape. The highest output was achieved with shapes that are mostly flat and concentrate any necessary steep geometry in small areas of the roof surface. Roof shapes with larger, less steep valley areas did less well; the lower solar insolation is the result of more self shading. This is illustrated in Figure 11.
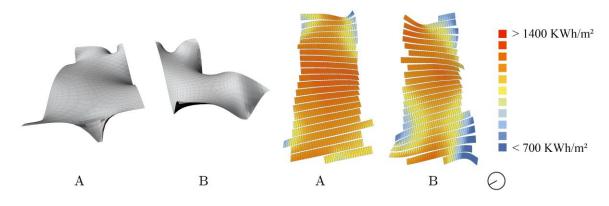

Figure 11: Two of the seventeen alternative roof shapes (left) and graphic display of solar insolation on these shells (right). Due to self shading and a less favourable orientation, geometry B has significantly lower solar insolation than geometry A.

3.2. Analysis of design parameters, as applied to case study roof

Using the methods described in section 2.1, 2.4, 2.5 and 2.6, we assessed the impact of relevant design parameters (panel dimensions and strip orientation) on solar insolation, panel bending and surface deviation of strips. This was done by evaluating the relevant metrics for every combination of the following parameters:

- Panel width: 0.3, 0.45, 0.6, 0.75 and 0.9 meter.

- Panel length: 1.2, 1.6, 2.0, 2.4 and 2.8 meter.

- Strip orientation: 13 angles, at 15° intervals.

In total, this resulted in data for 325 design alternatives. A detailed analysis of this data applied to one specific roof shape is presented in the following sections.

Surface area as a function of panel dimensions

The dimensions of the panels have a clear influence on the power output:

The available length for a strip is rarely an exact multiple of the panel length, so part of the available area will not be used. The size of the unused area depends on the angle between the panel and the edge, and on the panel length. On average, more than half a panel length of potential space is lost on each strip. Using shorter panels helps reduce these losses.

The effect of panel width on active surface area is clear: wider panels result in a smaller loss of potential roof area as there are fewer gaps between panels.

In practice, photovoltaic panels often have an inactive edge area. The losses caused by these edges are relatively strong for narrow and/or small panels. Still, for common panel sizes, short, wide panels result in the largest active PV surface in our case study, as can be seen in Figure 12.
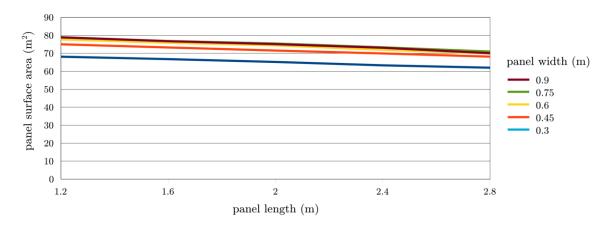
Figure 12: Achievable active module surface as a function panel length and width, assuming an inactive edge area of 1.5 cm wide.

Active panel surface area as a function of panel strip orientation

Certain strip orientations result in a denser arrangement of strips and thus in a larger active surface area than other orientations, as can be seen in Figure 13 (left). Long strips typically result in more variation in the width of gaps between panels, which may be due to the longer distances over which the gaps can accumulate, but also depends on the base geometry.

In our case study, the best results were achieved when orienting strips mostly perpendicularly to the longest roof edges (see Figure 13, right). As Figure 14 shows, the difference between various orientations is significant: almost 14%.
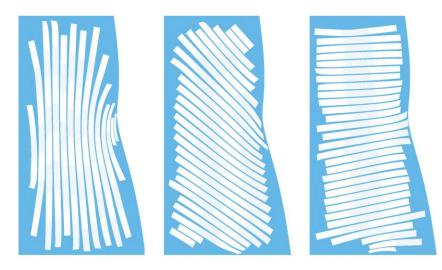

Figure 13: Strip arrangements using various starting angles. From left to right: 90°, -30° and 15°.
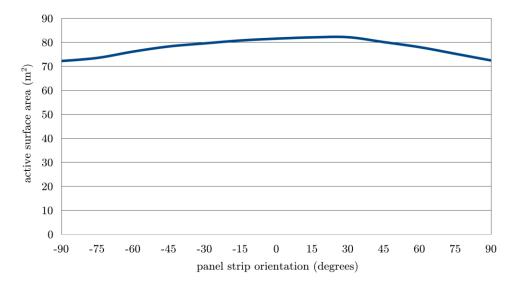
Figure 14: Average surface area as a function of strip orientation.

Strip bending as a function of strip orientation

On the topic of bending, considering the possible arrangements of strips on a cylinder shows that the strip orientation can have a large impact on the amount of bending within the strips as it can range from 0 (following the direction of the cylinder) to totally curved (following the circumference of the cylinder). The same thought experiment suggests that the width of the strips does not affect the amount of bending in the length direction of the strips.
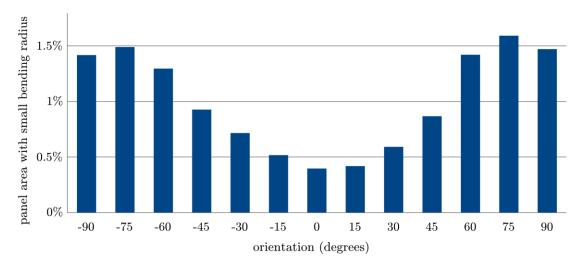

Figure 15: Occurrence of strong curvature for various strip angles: percentage of panel area that features bending at a small radius.

Analysis of the amount of bending occurring for various strip widths and orientations on our roof shape confirms the expected behaviour: the strip width does not significantly affect the amount of panel bending, but as shown in Figure 15, the orientation of the panels does.

Effect of panel dimensions on surface approximation accuracy

Strip width logically affects the accuracy with which the original surface can be approached. Using strips of 0.3 m wide, the distance between the original surface and the generated strips is less than 5 mm for most of the area and never larger than 20mm. However, as can be seen in Figure 16, the surface approximation is much less accurate when using wider panels. This has visual implications but also may affect the panel mounting system.
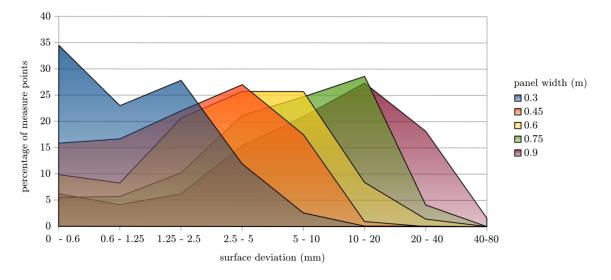

Figure 16: Surface deviation for strips of various widths.

3.3. Solar insolation

The amount of solar insolation does naturally depend on the surface area of the panel, so the results mentioned in 3.2.1 and 3.2.2 directly apply to solar insolation as well.

For the roof geometry we used, the orientation of the strips on the roof does not significantly affect the total annual insolation.

4. CONCLUSION

We have introduced geometric methods to approximate doubly curved geometry using triangulated strips, as well as methods to organise such strips efficiently on a surface. We combined these methods with solar insolation analysis software in order to facilitate design and analysis of bendable photovoltaic panels on irregularly curved surfaces.

Using this integrated tool chain, we analysed the solar insolation potential of various roof shell geometries in a case study project. We also studied the impact of various geometric parameters on potential solar insolation.

For the roof geometry we studied, the solar insolation is almost perfectly linearly dependent on the panel surface area. Short and wide panels that are oriented mostly perpendicularly to the longest edges of the roof resulted in the largest effective PV area and in the highest solar insolation. On the other hand, narrow panels result in less geometric deviation from the roof geometry.

The methods we introduced proved to work reliably and efficiently in our case study, despite the geometric complexity of the roof. This suggests that the methods work for a wide range shapes. Because the strip geometry generation and irradiance analysis are automated and take little time to calculate, the system described in this paper could potentially be combined with other automated design tools, such as structural form finding.

References

1. Rippmann, M., Lachauer, L. and Block, P., Interactive Vault Design, International Journal of Space Structures, 2012, 27(4), 219-230.

2. Williams, N., Stehling, H., Scheurer, F., Oesterle, S., Kohler, M. and Gramazio, F., A Case Study of a Collaborative Digital Workflow in the Design and Production of Formwork for 'Non-Standard' Concrete Structures, International Journal of Architectural Computing, 2011, 9(3), 223-240.

3. Schwinn, T., Krieg, O. and Menges, A., Robotically Fabricated Wood Plate Morphologies, in: Brell-Cokcan, S and Braumann, J. eds., Rob|Arch 2012, Springer, Vienna, 2013, 48-61.

4. Park, P., Gilbert, M., Tyas, A. and Popovic-Larsen, O., Potential use of structural layout optimization at the conceptual design stage. International Journal of Architectural Computing, 2012, 10(1), 13-32.

5. Scheurer, F., Materialising Complexity, Architectural Design, 2010, 80(4), 86-93.

6. Kolarevic, B., ed., Architecture in the Digital Age: Design and Manufacturing, Spon Press, New York, 2003.

7. Kidder, F.S., Triangulation Applied to Sheet Metal Pattern Cutting, The Sheet Metal Publication Company, New York, 1917.

8. Frey, W. H., Boundary Triangulations Approximating Developable Surfaces That Interpolate a Closed Space Curve, International Journal of Foundations of Computer Science, 2002, 13, 285-302.

9. Tang, K. and Wang, C.L., Modeling Developable Folds on a Strip, Journal of Computing and Information Science in Engineering, 2005, 5(1), 35-47.

10. Wallner, J., Schiftner, A., Kilian, M., Flöry, S., Höbinger, M., Deng, B., Huang, Q. and Pottmann, H., Tiling Freeform Shapes With Straight Panels: Algorithmic Methods, Advances in Architectural Geometry 2010, 2010, 73-86.

11. Díaz-Dorado, E., Suárez-García, A., Carrillo, C.J. and Cidrás, J., Optimal distribution for photovoltaic solar trackers to minimize power losses caused by shadows, Renewable Energy, 2011, 36(6), 1826-1835.

12. Gordona, J.M. and Wengera, H.J., Central-station solar photovoltaic systems: Field layout, tracker, and array geometry sensitivity studies, Solar Energy, 1991, 46(4), 211-217.

13. Choo, T. S. and Janssen, P., Evolutionary optimisation of semitransparent building integrated photovoltaic facades, International Journal of Architectural Computing, 2014, 12(1), 81-100.

14. Sun, L., Lu, L. and Yang, H., Optimum design of shading-type building-integrated photovoltaic claddings with different surface azimuth angles, <u>Applied Energy</u>, 2012, 90, 233-240.

15. Crawley, D.B., Pedersen, C.O., Lawrie, L.K. and Winkelmann, F.C., EnergyPlus: Energy Simulation Program, <u>ASHRAE Journal</u>, 2000, 42, 49-56.

16. Jakubiec, A and Reinhart, C.F., DIVA 2.0: integrating daylight and thermal simulations using Rhinoceros 3D, DAYSIM and EnergyPlus, <u>Proceedings of Building Simulation 2011, 12th Conference of International Building Performance Simulation Association</u>, IBPSA, Sydney, 2011, 2202-2209

17. Roudsari, M. S., Pak, M., and Smith, A., Ladybug: A Parametric Environmental Plugin for Grasshopper to Help Designers Create an Environmentally-Conscious Design, <u>Proceedings of Building Simulation 2013: 13th Conference of International Building Performance Association</u>, Chambery, IBPSA, 2013, 26-28.

18. http://www.grasshopper3d.com [23-02-2015].

19. ASHRAE, International Weather for Energy Calculations (IWEC Weather Files) Users Manual and CD-ROM, ASHRAE, Atlanta, 2001.

20. http://www.luxrender.net [23-02-2015].

21. http://hilo.arch.ethz.ch [23-02-2015].

22. Veenendaal, D. and Block, P., Design process for a prototype concrete shells using a hybrid cable-net and fabric formwork, <u>Engineering Structures</u>, 2014, 75, 39-50.